

WATER PERMEABILITY OF MEA FUEL CELL FABRICATION USING X-Y ROBOTIC SPRAYER

Ramli Sitanggang, Danang Jaya

- a. Fuel Cell Institute, Universiti Kebangsaan Malaysia, 43600 UKM, Bangi, Selangor, Malaysia
- b. Teknik Kimia, FTI, UPN "Veteran". Jl. SWK 104 Condongcatur, Yogyakarta, Indonesia, 55283

Abstract

The fabrication of MEA is conducted using an in-house robotic sprayer machine capable of adjusting its X-Y motions. The MEA produced was analyzed for porosity; distributions pore and water flux using BET and SEM based on the water permeability methodology. The results of the MEA shown that the pore geometry of MEA has a tortuosity parameter which is greater than the MEA's thickness while the permeability coefficient parameter of water is $9.10^{-5} \text{ gcm}^{-1}\text{men}^{-1}\text{psia}^{-1}$ or the tortuosity of 2. These results were then compared to the ones available from the commercial MEA.

Keywords: permeability coefficient, membrane electrode assembly

1. INTRODUCTION

Membrane Electro Assemblies (MEA) is the core component of fuel cell. It consists of the electrolyte membrane, anode and cathode electrodes. The electrochemical reactions occur when a fuel and oxidant are applied to the anode and cathode sides of the MEA. There are several fabrication methods of MEA were reported, such as rolling, screen-printing, casting, and spraying. Each of these types produces different MEA's structure. One of the recent researches in sprayer as what we interested in our laboratory, used one or multi nozzle (Chun, 2001). The most important parameter in MEA is the water flux, usually named as water transport phenomenon. The water flux itself depends on electro – osmotic behavior, diffusion and permeability coefficient, and proton movement (Eikerling, 1998, Hu, 2004). Some of researchers have approached the water transport phenomenon in one, two and three dimensional (Hu, 2004, Chen, 2003). Based on the mechanism of hydrogen bridge within membrane (Bansal,1998), we observed that the water flux is pressure dependent. The balancing of humidity has to be insured with avoiding the floods of water and dehydration that will cause an ohmic lost. The minimizing of ohmic lost was suggested by many researcher by achieving various composition of materials and reconstruction of pore size of diffusion layer of electrode. In this research, we observed the permeability coefficient of MEA by setting the slope of water flux in a certain value.

2.THEORY

MEA consists of three component Gas Diffusion Layer (GDL), Gas Diffusion Electrode (GDE), and membrane. The fabrication process of GDL and GDE was made using in-house robotic sprayer machine adopted the Chun's method (2001). The permeability coefficient of the fabricated electrodes was characterized. We are assuming the water mass transfer represents by the simplest equation as follows (Middleman, 1997, Muider, 1991, Baker,200, Frank,2004):

$$N = \kappa \cdot \Delta P_{eff} \quad (1)$$

Where K is the membrane permeability coefficient that depends on the porosity, pore radius, viscosity and turtocity factor, effective pressure difference (ΔP_{eff}) and N permeate flux. The System configuration in our study is an in-house robotic sprayer was in house fabricates. Data of work piece is computer controlled. The post processor converts the spray coating carbon ink path-line to the robot control command to move the sprayer in X-Y direction. Such spraying system will produce an even GDL. The GDE is produced by spraying the GDL with a similar process as mentioned above but with difference formula of ink-platinum. The produced MEA is subjected to hot pressing in a sandwich form of GDE with membrane inside in high temperature and high pressure (Chun, 2001). After that we activate the MEA using treatment method (Kwak,

2000), and then boiled it to avoid water and gases inside the pore. MEA was characterize the dimension of pore of MEA, GDL and GDE using BET and SEM by analyzing the permeate and the slope of water flux. The analyzed permeate was done using continuous membrane system method and the analyzing of the slope water flux by linear fitting curve against pressure difference as presented in Eq.(1). Permeability coefficient and MEA performance was investigated using FCTS.

The robot used in the system employs a specific attitude expression of the x-y configuration shown in Fig 1.

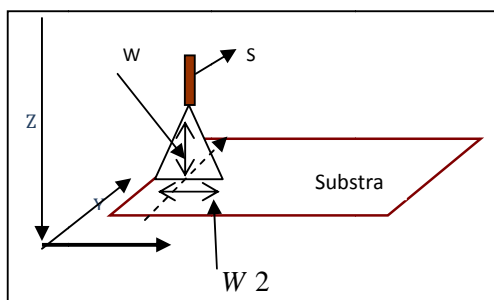


Fig 1. The x-y configuration

The spray variable is expressed by frequency (ω), nozzle height (W_1), distribution distance (W_2), division number of spray coating line on substrate (n) and nozzle velocity (S). The spray direction coating process is designed perpendicular to substrate. If thick size (t_e), pore diameter (d_p), porosity (ε), typical activated specific surface (a_s). The variable of ink drop distribution of the nozzle will affect the layer size are μ , ν and p .

$$t_e, d_p, \varepsilon, a_s = f(K, \mu, \nu, \sigma, p) \dots\dots\dots 3$$

Assume p is constant, surface tension (σ) constant, thus theoretically the correlation of t_e , d_p , ε , and a_s toward all variables and the robotic movement as well as the drop variable are given by dimensionless equation 4

$$t_e, d_p, \varepsilon, a_s = f(N_{spray}, Re, W) \dots\dots\dots 4$$

The viscosity effect and surface tension are constant and neglecting the solidifying effect on substrate surface. Based on equation 3, the t_e , d_p , ε , a_s are given by the dimensionless equation 4 to 5, as follows :

$$t_e, d_p, \varepsilon, a_s = f(N_{spray}) \dots\dots\dots 5$$

Equations 4 to 5, the t_e , d_p , ε and a_s of an electrode can be determined by the robotic characteristic number (N_{spray}). Assumed the layers results from robotic sprayer is set to be the MEA, therefore the relationship of N with the current density of PEM fuel cell can be formulated using Grujicic (2004) . The spraying technique model for MEA fabrication is as follows:

Current density (i):

$$i = K_4 C_{O_2} (1 - (K_5 \exp(-K_6 (\phi_s)))^{1/2}) \dots\dots\dots 6$$

$$x \coth(K_5 \exp(-K_6 (\phi_s)))^{1/2}$$

$$K_4 = \frac{12 t_e (1 - \varepsilon) F D_{O_2}}{0.5 d_p} = f(N_{spray}) \dots\dots\dots 7$$

$$K_5 = \frac{i_{0,c} a_{s1} (0.5 d_p)^2}{4 F C_{O_2}^{ref} D_{O_2}} = f(N_{spray}) \dots\dots\dots 8$$

and Voltage (V):

$$V =$$

$$E - \frac{RT}{0.5F} \ln \{ f_1(dp, \varepsilon) C_{O_2} (1 - (f_1(dp, \varepsilon) \frac{i_{0,c}}{C_{O_2}^{ref}} \exp(-\frac{RT}{0.5F} (\phi_s)^{1/2}) x \dots \dots \dots 9$$

$$\coth(f_1(dp, \varepsilon) \frac{i_{0,c}}{C_{O_2}^{ref}} \exp(-\frac{RT}{0.5F} (\phi_s)^{1/2}) / i_{o,c}$$

Based on equations, the value of coefficient model of current density depend on N_{spray} . The N_{spray} becomes the main control for manufacturing layer size of MEA design form

Generally, the MEA design form configuration employed by researches as shown in Fig.3a is the G-GDL-E-M-E-GDL-G. In this paper the catalyst layer employed the configuration as shown in Fig.3b to obtain highly activated specific surface area. In Fig.3c the catalyst utilised a support to composite the catalyst into the membrane (novel).

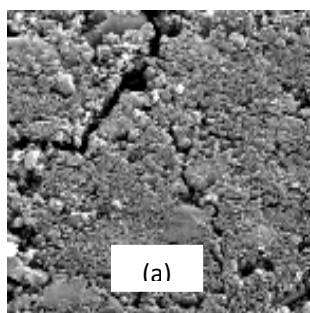
3.EXPERIMENT

Active carbon with 400 meshes was laminated on carbon cloth. Polytetrafluoroethylene (PTFE), Nafion liquid was used also. Moderately polar of mix solvent from water and isopropanol was used as medium for carbon mobilition, and the membrane used in this observation is nafion 117 produced by DuPont. The fabrication process of MEA consists of three steps; the laying of GDL, GDE, membrane activation and assembly of membrane electrodes (MEA). In the GDL fabrication layer mixture of activated carbon, alcohol, water, Nafion and PTPE are stirred for 10 minutes. The slurry produce has viscosity for about 1.17 cp and usually called as carbon ink. The carbon ink is sprayed on carbon cloth with flow of spraying as 0.5 ccs, 6 bar air pressure through spraying nozzle, with pattern of 4 cm, and the standing position of nozzle is perpendicular with the object, with 10 times moving period. The fabricated GDL must be dried using vacuum dryer in room temperature for about 2 hours, and then will be subjected to BET, SEM and permeate test characterization. The profile and permeability coefficient of the material was test also. In case of the fabrication of GDE, the GDL must be sprayed with another mixed material that consists of C-Pt, water, and alcohol. Nafion, PTPE. The materials must be mixed for 5 minutes, and the result is namely as carbon ink C-Pt and has 1.16 cp viscosity. The procedures of spraying after mixing process are similar as above.

The third material that we used is membrane Nafion 117. Membrane were cleaned to remove any trace of impurities and stored in deionized water further use. The MEA, GDE and membrane will sandwich together using hot press. The produces electrode will be rinsed with 0.5 M H_2SO_4 and have to be dried in vacuum dryer in room temperature for 2 hours. The result then has to be characterized using permeability test and FCTS.

4.RESULT AND DISCUSSION

Characterization. The fabrication process of GDE was repeated seven times in insure reproductability. Surface scanning was done using SEM have produced to characterized the crack and the roughness of the GDE surface. From the SEM characterization of experimental 1 to 6 (see Fig. 2a), the results still has crack, and in experimental (see Fig. 2b) the result is free of crack. Experimental (b) also has similar surface roughness with commercial GDE (see Fig. 2c). Matrix morphology was investigated for particles characterization BET studies was performed and reveal



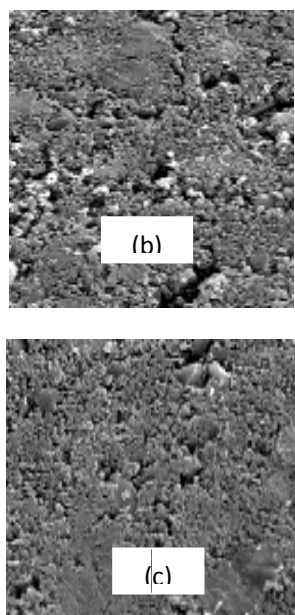


Fig. 2 Surface microscope scanning of (a). First trial (b). After modified, (c). Reference electrode

Table 1. BET analysis

Property	GDE (a)	GDE (b)	ME A (a)	MEA (b)	ME A (c)
Diameter pore (\AA)	34.3 1	41.15	34.4 1	39.41	68.2
Surface area (m^2/g)	472	451	410	450	220
Volume pore (cc/g)	0.09 7	0.157	0.06 0	0.102	0.08 1

For the next observation, we will focus on experimental (b) that has activated carbon as 1.05 g cm^{-2} and 0.53 g cm^{-2} PTFE, 0.51 g cm^{-2} C-Pt and the scale characteristic as mentioned in Table 1. Using pore dimension point of view within micropore scale, experimental (a) and (b) have mesopore characteristics (Ruthven, 1997). Another advantage of experimental (b) is that it has greater adsorption capacity and pore capability than the other experimental in our observation. After assembly the membrane with electrode of experimental (b), the pore dimension of MEA remains similar with GDE experimental (b) stand alone. We could conclude that the experimental (b) is appropriate as a material for fabricating fuel cell.

Permeability Coefficient. Within MEA fuel cell, the GDL has a function to distribute humidity water and evacuate water from electrode part, meanwhile the electrode is used to distribute humidity water and will use for triggering the reaction between Pt and CO. The membrane also has task to bond water for bridging hydrogen and sweeping out the electron (Mikko, 2003). If we flow water through the layers within MEA, then the water flux inside each layer will depend on the channel structure.

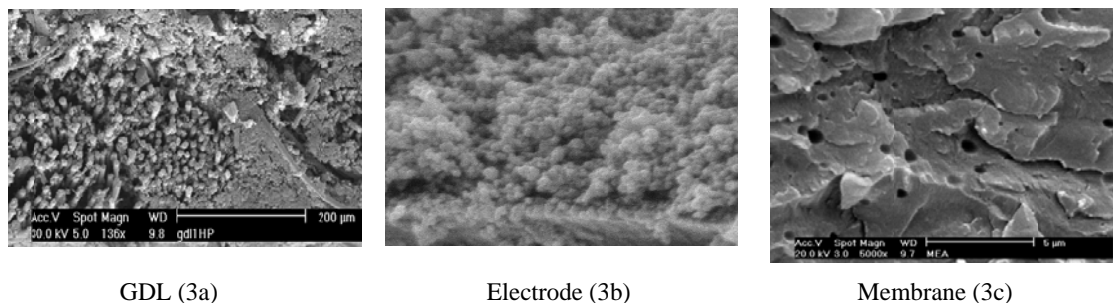


Fig 3. Surface of GDE

For GDL, the water flux will be affected by channel that has been built within the carbon cloth (see Fig. 3a), meanwhile the water flux inside the electrode will be affected by channel that has been built by the mesopore.

Figure 3c illustrates good profile of pore within membrane to make possible water flux flow through it. Such kinds of pore profile are usually called as porosity and tortuosity. To build better understand about what we mentioned above, we will explain more detail about the capability of MEA to flow water flux as follow

$$N = 3.10^{-4} \Delta P_{eff} \quad (2)$$

$$N = 10^{-4} \Delta P_{eff} \quad (3)$$

$$N = 2.10^{-4} \Delta P_{eff} \quad (4)$$

Eq. (2) is developed from eq. (1) with κ for about $3.10^{-4} \text{ gcm}^{-1} \text{men}^{-1} \text{psia}^{-1}$ that has been found using Figure 4, and ΔP_{eff} indicates the pressure differences of water flux. Using tortuosity table we got 1.1 for 3.10^{-4} permeability coefficient. It means that the length of channel for flowing water within GDL is greater than the thickness of GDL itself. Furthermore, for calculating the capability of electrode to flow water follows eq. (3) as shown in Figure 4b. With $10^{-4} \text{ gcm}^{-1} \text{men}^{-1} \text{psia}^{-1}$ of permeability coefficient it is similar with 1.7 tortuosity. It also means that the channel for flowing water within electrode greater than the thickness of electrode itself. From the calculation of water flux as mentioned above, we could emphasize that the flow resistance of water within electrode is greater than within GDL. It means that GDL is capable to distribute and evacuate water easier and electrode could flow in or out water faste

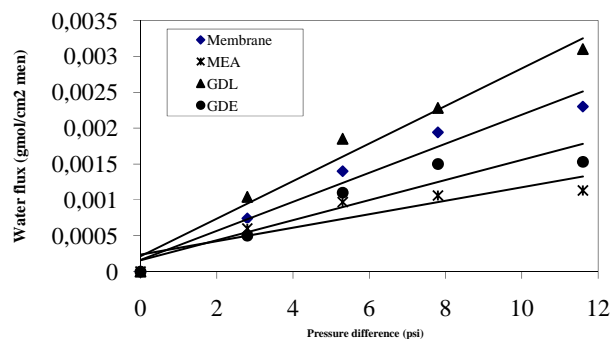


Fig 4. Characteristic Permeability Water

For calculating the water flux within membrane Nafion 177, we use eq. (4) with permeability coefficient of $2.10^{-4} \text{ gcm}^{-1} \text{men}^{-1} \text{psia}^{-1}$ or 1.4 tortuosity, it means that the channel length within membrane is also greater than its thickness. From these three layers discussed above, we could conclude that water resistance as follows

$$\text{GDL} < \text{membrane} < \text{electrode} \quad (5)$$

After assembly of membrane and electrodes on 35 kgfcm^{-2} pressure and 130°C temperature, we get water flux as in eq. (6).

$$N = 9.10^{-5} \Delta P_{eff} \quad (6)$$

The capability of MEA to distribute water is proportional with the pressure difference that is attached to MEA. With 2.8 psia pressure differences, MEA could flow water around $3.3 \cdot 10^{-5} \text{ gmol cm}^{-2} \text{ min}^{-1}$ and restore around $3.6 \cdot 10^{-4} \text{ gmol cm}^{-2}$. The permeability coefficient of water within MEA is around $9 \cdot 10^{-5} \text{ gcm}^{-1} \text{ men}^{-1} \text{ psia}^{-1}$ or with tortuosity greater than 2. Therefore we could modify eq. (5)

$$\text{GDL} < \text{membrane} < \text{electrode} < \text{MEA} \quad (7)$$

Electrode has greatest water resistance, it means that to fabricate MEA, we have to modify electrode layer to control the water distribution and evacuation properties. Including the commercial MEA (with $2 \cdot 10^{-6} \text{ gcm}^{-1} \text{ men}^{-1} \text{ psia}^{-1}$ permeability coefficient), eq. (7) will have to modify to

$$\text{GDL} < \text{membrane} < \text{electrode} < \text{MEA} < \text{MEA Com} \quad (8)$$

4.3. Permeability experiment related to performance of MEA fuel Cell

In observing the MEA fuel cell with single stack, pressure at anode is set up greater than the pressure of oxygen. With pressure difference of 2.8 psi and flow rate of H₂ as 0.3 slpm, oxygen 0.4 slpm and a flooding water is happened within membrane, then the performance of MEA fuel cell could be illustrated as in Figure 5.

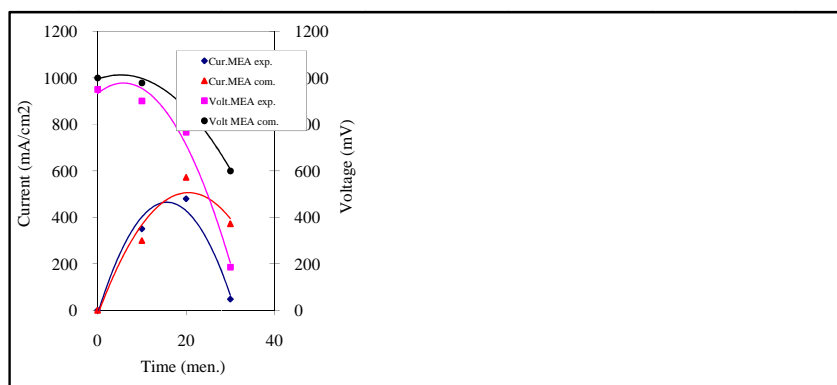


Fig 5. Characteristic Performance MEA fuel Cell

As can be seen in Figure 5, the MEA fuel cell with greater permeability coefficient will have less current density voltage. In this operation, the anode MEA fuel cell will be dehydrated and osmotic electron will be happened through the membrane. This osmotic electron or usually called as electron diffusion will cause ohmic losses inside the MEA fuel cell. In such condition, the changing of current within MEA tends to drop rapidly than the commercial MEA for 30 minutes operation times. This difference is due to the permeability coefficient of our MEA greater than the commercial MEA. If H₂ and O₂ suddenly drop out to zero, the MEA current will be discharged very rapidly than the commercial MEA. It means that MEA with very rapidly transient current (rise time and fall time) is good enough to control dehydration in low temperature without any drying process (Savadogo, 2003)

5.CONCLUSION

From the discussion above, the water flux within the geometrical structure of MEA is influenced strongly by porosity and tortuosity. The tortuosity of the layer could be defined as $\text{GDL} < \text{membrane} < \text{electrode}$ or we got the permeability coefficient of DGL as $3 \cdot 10^{-4} \text{ gcm}^{-1} \text{ men}^{-1} \text{ psia}^{-1}$, Electrode as $10^{-4} \text{ gcm}^{-1} \text{ men}^{-1} \text{ psia}^{-1}$ membrane as $2 \cdot 10^{-4}$, MEA as $9 \cdot 10^{-5} \text{ gcm}^{-1} \text{ men}^{-1} \text{ psia}^{-1}$ or tortuosity greater than 2 for MEA. The MEA will occur ohmic losses using greater permeability coefficient.

ACKNOWLEDGEMENTS

The authors would like to express their gratitude to the UKM University and Environment of Malaysia for the financial support through IRPA grant: IRPA 02-02-02-0003-PR0023 11-08



REFERENCE

- Midleman, S. An Introduction to mass and heat transfer. John Wiley & Sons, Inc (1997)
- Ruthven D. Encyclopedia of Separation Technology. Vol 1., John Wiley, New York (1997)
- Baker W.R. Membrane technology and Applications. McGraw-Hill (2000)
- Chun, William et al. Direct deposit of catalyst on the membrane of direct fuel cell. California Institute of technology, California corporation (2001)
- Muider M. Basic Principles of Membrane Technology. Center for membrane Science and Technology, Universities of Twente, the Netherlands (1991)
- Mikkola, Helsinki University of Technology (2003)
- Frank M., Gerhart E. Transport parameter for modeling of water transport ionomer membrane for PEM Fuel Cell. Electrochemical Acta in press (2004)
- Besset, J. et al. A Textbook of Quantitative Inorganic Analysis. Logman Group Limited London (1987)
- Bansal, Raj K. Organic Reaction Mechanisms. Tata McGraw-Hill Publishing Company Limited (1998)
- Eikerling, Yu.I. Kharkats, A.A., Kornyshe, Volkovich, J. Electrochem. Soc. 145 (1998) 2684
- Hu M., Zhu X., Wang M, Gu A., Yu L. Three dimensional, two phase flow mathematical model for PEM Fuel cell: Part II. Analysis and discussion of the internal transport mechanisms. Energy and management, Published by Elsevier Ltd, in press (2004)
- Kwak S.H., Peck D.H.. New Fabrication method of the composite membrane for polymer electrolyte membrane fuel cell. J. New Mat. Electrochem systems, 4, 25-29 (2001)
- Chen F. Transient behavior of water transport in the membrane of a PEM fuel Cell. Journal of Electroanalytical Chemistry in press (2003)
- Grujicic & Chittajallu K.M. 2004. Design and optimization of polymer electrolyte membrane (PEM) fuel cells. Applied Surface Science 227: 56–72